THE ASTROPHYSICAL JOURNAL, 456:686–695, 1996 January 10

POTENTIAL PROTOSTARS IN CLOUD CORES: H_2CO OBSERVATIONS OF SERPENS

ROBERT L. HURT AND MARY BARSONY
Department of Physics, University of California, Riverside, Riverside, CA 92521; rhurt@fun.ucr.edu, fun@nusun.ucr.edu
AND
ALWYN WOOTTEN
NRAO,[1] 520 Edgemont Road, Charlottesville, VA 22903-2475; awootten@nrao.edu
Received 1995 March 27; accepted 1995 July 20

ABSTRACT

The Serpens cloud contains a large number of heavily embedded protostellar cores. We present results of a formaldehyde survey of the strongest submillimeter continuum sources here in an attempt to determine the gas properties in these objects. The formaldehyde transitions we have measured trace exceptionally dense gas to which most other commonly observed molecular species, or dust, are not sensitive. In the four sources observed in at least three H_2CO transitions, we find higher gas kinetic temperatures than have been derived previously, ranging from 40 to 190 K. The gas densities in this region are also large, in the range of $n_{H_2} \sim 10^6$–$10^{6.5}$ cm^{-3}. Some of the objects exhibit strong self-reversal features that may indicate infall, and two of them possess exceptionally broad line wings, which may be associated with molecular flows. Several of these sources may represent extremely young protostars that have not yet accreted the bulk of their mass from their surrounding circumstellar envelopes.

Subject headings: circumstellar matter — ISM: clouds — ISM: individual (Serpens) — radio lines: ISM — stars: formation — stars: pre–main-sequence

1. INTRODUCTION

The very earliest protostellar stage has recently been observationally characterized and dubbed "Class 0" (André, Ward-Thompson, & Barsony 1993; Barsony 1994). Physically, such a system consists of a central object, often evident as a weak centimeter continuum source, which has yet to accrete the bulk of its "initial mass" as a star from its surrounding infall envelope. The cool, dense gas and dust of that envelope thus dominates the spectral energy distribution observed toward the nascent star. The ultimate luminosity source that powers these objects remains unclear, but the hot gas whose presence is signaled by the centimeter-wave emission suggests that either shock ionization of surrounding gas by a stellar wind (Anglada et al. 1992) or inner accretion shocks (Bertout 1983) contribute. Although these deeply embedded Class 0 sources already power molecular outflows, they are observationally distinguished from the later Class I phase by large submillimeter/bolometric luminosity ratios, spectral energy distributions that resemble a pure blackbody at $T \leq 30$ K, and invisibility at wavelengths less than 10 μm (Barsony 1994). Because of their extreme youth (approximately a few $\times 10^4$ yr), such sources are rare, amounting to only 1% of the stellar population of any embedded, young pre–main-sequence cluster (Fletcher & Stahler 1994a, b). Ongoing searches for new objects of this class consist of combinations of near-infrared, submillimeter continuum, centimeter continuum, and molecular-outflow surveys of young, embedded star clusters.

The Serpens cloud core is one of the most spectacular examples of a protostellar nursery, harboring a stellar density that exceeds 450 stars pc^{-3} (Eiroa & Casali 1992). At a distance of 310 pc (de Lara, Chavarria-K., & López-Molina 1991), recent near-infrared (NIR) and submillimeter continuum surveys of the region have uncovered over a half-dozen millimeter/submillimeter continuum peaks among the more than 50 stars identified in the core, most of which *lack* NIR counterparts (Casali, Eiroa, & Duncan 1993; White, Casali, & Eiroa 1995). These embedded sources are prime Class 0 candidates.

We report the results of a preliminary multitransition H_2CO study of the millimeter/submillimeter emission peaks in Serpens in order to characterize the physical conditions of the associated gas. We have chosen H_2CO as our molecular probe since many of the most commonly used molecular tracers (such as CO, CS, and NH_3) are not adequate to the task of the probing of conditions in the potentially cold ($T = 10$–40 K), dense ($n = 10^7$–10^8 cm^{-3}) gas we expect to find in the youngest protostellar sources (Wootten 1988). The lower transitions of CO become optically thick before they probe deeply into the core's interior—even $C^{18}O$ $J = 2$–1 is optically thick in Class 0 sources. Formaldehyde (H_2CO) pervades the interstellar medium at high abundance, it does not show large abundance variations over a density range from 10^5 to 10^7 cm^{-3}, and its abundance does not vary much spatially, even in the chaotic OMC1-KL region (Mangum et al. 1990). Being a slightly asymmetric rotor, the H_2CO molecule exhibits many transitions in the submillimeter spectral range that are closely spaced in frequency, although they are substantially separated in energy. This fact allows the nearly independent determination of gas temperatures and densities by use of judiciously chosen line ratios. The exploration of physical conditions and kinematics of the earliest protostellar stage and of prestellar condensations with the rich millimeter/submillimeter spectrum of formaldehyde is just beginning, with encouraging results (Mangum & Wootten 1993; Helmich et al. 1994; Barsony et al. 1995; Mangum, Latter, & McMullin 1995).

In § 2, we describe our observations and data reduction. We outline our large velocity gradient (LVG) modeling of the

[1] The National Radio Astronomy Observatory is operated by Associated Universities, Inc., under cooperative agreement with the National Science Foundation.

various H_2CO line ratios in § 3 and report the derived gas temperatures and densities toward the recently discovered millimeter continuum sources. We conclude with a discussion of the nature of each source and make suggestions for future observations in § 4.

2. OBSERVATIONS

Observations of four H_2CO transitions toward millimeter continuum sources in Serpens were made with the Caltech Submillimeter Observatory's (CSO)[2] 10.4 m antenna, near the summit of Mauna Kea, Hawaii, during the nights of 1993 May 8–13. The SIS receiver that was employed is described by Ellison et al. (1989). The back end used consisted of two acousto-optical spectrometers (AOS): the high-resolution AOS, which consists of 1024 49 kHz channels with a 50 MHz bandwidth, and the low-resolution AOS, with 1024 channels separated by 0.54 MHz over a 500 MHz bandwidth. The four observed H_2CO transitions were 3_{03}–2_{02} (218.222192 GHz), 3_{22}–2_{21} (218.475632 GHz), 5_{05}–4_{04} (362.736048 GHz), and 5_{23}–4_{22} (365.363428 GHz). These moderately high excitation lines were specifically chosen to probe warm, dense gas thought to lie near the accreting object in our target sources. Other detected lines, which fell into our bandpass but will not be discussed further, were CH_3OH 4_2–3_1 (E) (218.4400 GHz) and HNC 4–3 (362.6301 GHz). Only the 218.222 GHz H_2CO line could be observed in the high-resolution 50 MHz AOS. In order to fit the two pairs of H_2CO lines (in the 218 GHz and 360 GHz bandpasses) into one observation each, we used the 500 MHz AOS.

Observing conditions were excellent to good, with $0.03 \leq \tau_{225\ \mathrm{GHz}} \leq 0.15$ throughout all observations, as measured by NRAO's tipping radiometer. Typical system temperatures were $T_{\mathrm{SSB}} \sim 500$ K at 218 GHz and 1100 K at 360 GHz. Standard chopper-wheel calibration was used to derive the T_A^* intensity scale (Ulich & Haas 1976; Kutner & Ulich 1981). The data were brought to the T_R scale by division of T_A^* by η_{MB}, the main-beam efficiency, measured to be 0.71 at 218 GHz and 0.55 at 365 GHz from observations of Jupiter (Mangum 1993). The CSO beam (FWHM) is 30″ at 218 GHz and 19″ at 363 GHz. Pointing was checked often and varied less than 5″ between measurements.

We observed seven sources in the Serpens cloud core, six of which have been detected as millimeter/submillimeter continuum sources ("SMM" designates an identification by Casali et al. 1993): FIRS 1 (also SMM 1), S68N (first identified by McMullin et al. 1994; also designated SMM 9 by White et al. 1995), SMM 2, SMM 3, SMM 4, IRS 53 (also SMM 5; weak in the submillimeter continuum), and SVS 2 (no detected submillimeter continuum). Our H_2CO line detections are listed in Table 1, and the corresponding high-resolution spectra are shown in Figure 1*a* (arranged from strongest to weakest). The

[2] The CSO is supported by NSF grant AST 9313929.

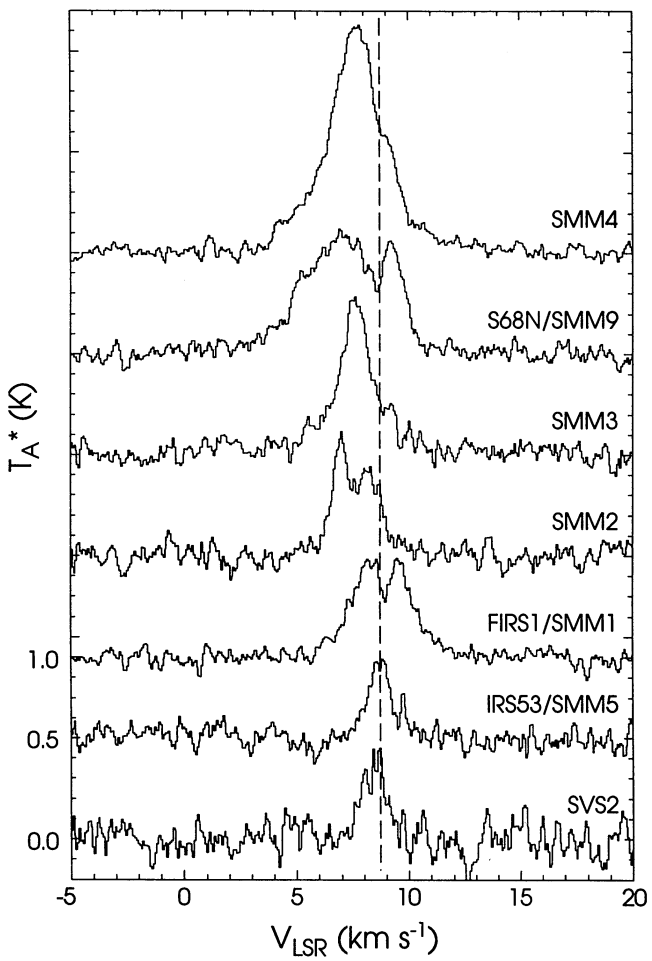

FIG. 1*a*

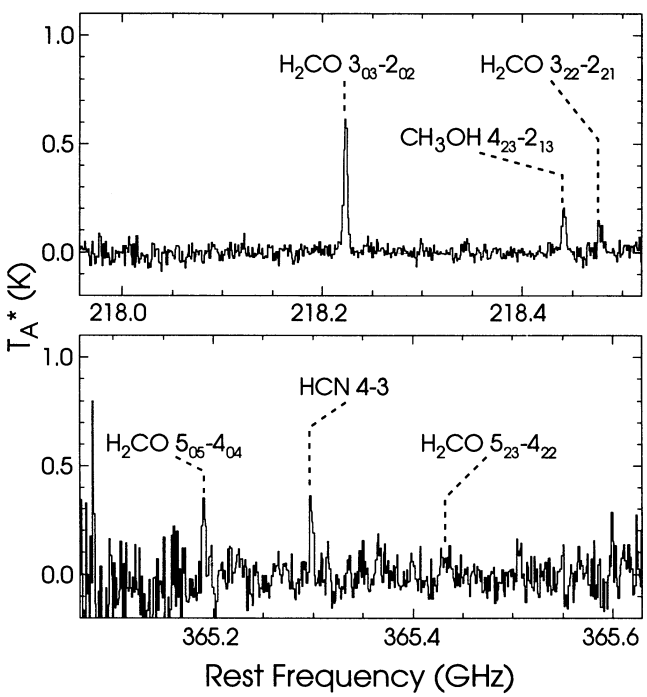

FIG 1*b*

FIG. 1.—Serpens H_2CO spectra presented in units of T_A^* (K). (*a*) H_2CO 3_{03}–2_{02} (218.222 GHz) high-resolution spectra for all of the observed Serpens sources. The spectra are offset from one another in 0.5 K increments for clarity of presentation. (*b*) Representative 218 and 365 GHz band low-resolution spectra (in this case, for the source S68N). The vertical dashed line at $v_{\mathrm{LSR}} = 8.75$ km s^{-1} helps to illustrate the location of the absorption features in SMM 4, S68N, SMM 3, and FIRS 1 with respect to the velocity centroid of the emission from the ambient cloud, as detected at the positions of IRS 53 and SVS 2.

TABLE 1

SERPENS H_2CO OBSERVATIONS

SOURCE	POSITION (1950) R.A.	POSITION (1950) decl.	H_2CO 3_{03}–2_{02} LINE $\int T_R dv$ (K km s^{-1})	v_{sys} (km s^{-1})	v_{width} (km s^{-1})	H_2CO LINE PEAK T_R 3_{03}–2_{02} (K)	3_{22}–2_{21} (K)	5_{05}–4_{04} (K)	5_{23}–4_{22} (K)
FIRS 1/SMM 1.....	$18^h27^m17^s.3$	1°13′23″	2.17	8.80	2.56	0.75 ± 0.07	0.25 ± 0.07	0.84 ± 0.18	0.36 ± 0.18
S68N/SMM 9.....	18 27 15.2	1 14 57	4.07	7.24	3.87	0.90 ± 0.06	0.16 ± 0.06	0.73 ± 0.20	0.33 ± 0.20
SMM 2.....	18 27 20.0	1 10 45	1.60	7.58	1.71	0.52 ± 0.10	<0.21 ± 0.10	...	...
SMM 3.....	18 27 27.3	1 11 55	2.71	7.62	2.28	0.73 ± 0.06	0.10 ± 0.06	0.44 ± 0.18	<0.27 ± 0.18
SMM 4.....	18 27 24.7	1 11 10	5.22	7.57	3.61	1.40 ± 0.04	0.33 ± 0.04	0.65 ± 0.13	<0.27 ± 0.13
IRS 53/SMM 5.....	18 27 18.9	1 14 36	0.77	8.74	1.09	<0.21 ± 0.18	<0.21 ± 0.18	...	...
SVS 2.....	18 27 25.4	1 12 41	1.00	8.38	0.68	<0.21 ± 0.17	<0.21 ± 0.17	<0.27 ± 0.22	<0.27 ± 0.22

continuum sources all have significantly stronger profiles than IRS 53 and SVS 2 and exhibit non-Gausian features. IRS 53 and SVS 2 are both associated with NIR sources; their H_2CO lines are relatively weak and nearly Gaussian. Since they do not appear as distinct sources in 3_{03}–2_{02} maps of this region (Mangum et al. 1995), we take them to be representative probes of the ambient medium near the continuum sources (SMM 5 is within 1′ of both FIRS 1 and S68N whereas SVS 2 is within 1.′5 of SMM 3 and SMM 4). All sources were observed at 218 GHz, but the higher frequency transitions, necessary for determination of density, were obtained only for FIRS 1, S68N, SMM 3, and SMM 4, all of which lack NIR counterparts and qualify as Class 0 candidates. Representative low-resolution spectra for S68N are presented in Figure 1*b*.

To isolate the cooler gas component of the cores, we obtained additional spectra of the H_2CO 1_{01}–0_{00} line at 72.83795 GHz and its optically thin $H_2{}^{13}CO$ 71.0248 GHz counterpart toward FIRS 1, S68N, and SMM 4 at the 12 m telescope of NRAO in 1994 September. The primary beam has a 90″ FWHM with a main-beam efficiency of 0.65 at these frequencies. The velocity resolution of these observations was 0.422 km s^{-1} per channel, over 128 channels.

3. DATA ANALYSIS

We determine the gas conditions in the Serpens submillimeter sources via a large velocity gradient (LVG) model, similar to the methods of Mangum & Wootten (1993). The LVG code gives the gas radiation temperature as a function of three parameters: the gas kinetic temperature T_K, the gas density n_{H_2}, and the column density per unit velocity interval, $N(\text{para-}H_2CO)/\Delta v$. For a given source, we first estimate $N(\text{para-}H_2CO)/\Delta v$ given the observed peak line strengths. The top panels of Figure 2 illustrate how isosurfaces derived from the LVG model for the observed line strengths of S68N converge at a narrow set of column density values; the other sources show similar behavior.

Fixing $N(\text{para-}H_2CO)/\Delta v$, we then find the best values in T_K-n_{H_2} parameter space to fit the observed ratios of peak line intensity $R_{33} \equiv T_R(3_{03}–2_{02})/T_R(3_{22}–2_{21})$, $R_{55} \equiv T_R(5_{05}–4_{04})/T_R(5_{23}–4_{22})$, and $R_{35} \equiv T_R(3_{03}–2_{02})/T_R(5_{05}–4_{04})$. The first two ratios are primarily sensitive to variations in T_K while the last is most sensitive to variations in n_{H_2}. The bottom panels of Figure 2 illustrate the isosurfaces through the parameter space that corresponds to the observed line ratios of S68N. It is clear from Figure 2 that the temperature and density parameters are not sensitive to small deviations in $N(\text{para-}H_2CO)/\Delta v$, which might result from errors in absolute calibration or small areal filling factors. The R_{33} and R_{55} ratios are free of such errors since each pair of lines appears within the same bandpass; only the density-sensitive R_{35} is subject to these uncertainties.

Our best fits are determined by minimizing χ^2 residuals of the form

$$\chi^2 = \sum_i \frac{[R_i(\text{obs}) - R_i(\text{LVG})]^2}{\{\sigma[R_i(\text{obs})]\}^2},$$

where R_i(obs) and R_i(LVG) are the corresponding observed and LVG model ratios and $\sigma[R_i(\text{obs})]$ is the standard error of the observations, all summed over the three defined ratios. Our minimizations are performed with three ratio observations to fit two variables, which leaves one degree of freedom. Surface plots of the χ^2 minimization parameter spaces are presented in Figure 3, and the results are summarized in Table 2.

TABLE 2

H_2CO GAS PROPERTIES

SOURCE	WARM GAS T_K (K)	WARM GAS log $n(H_2)$ (cm^{-3})	WARM GAS log N(para-H_2CO) (cm^{-2})	WARM GAS χ^2	COLD GAS[a] Δv (km s^{-1})	COLD GAS[a] log $n(H_2)$ (cm^{-3})	COLD GAS[a] log N(para-H_2CO) (cm^{-2})
FIRS 1[b].....	$190^{+>200}_{-90}$	$6.1^{+0.3}_{-0.2}$	12.86 ± 0.7	0.1	2.6	5.48	13.36
S68N.....	75^{+50}_{-25}	$6.4^{+0.4}_{-0.5}$	12.94 ± 0.7	0.4	3.1	5.48	13.39
SMM 3.....	40^{+110}_{-15}	$6.5^{+>1.5}_{-0.7}$	12.56 ± 0.7	[c]	2.3	5.48	13.23
SMM 4.....	85^{+20}_{-15}	$6.0^{+0.1}_{-0.2}$	12.92 ± 0.7	[c]	2.5	5.48	13.48

[a] Cold-gas temperature (20 K) and density are assumed.

[b] FIRS 1 is known to have a significant self-reversal at the line *center*, which could seriously affect the calculated temperatures and densities; the errors indicate that it also has the least well-determined parameter space of the four sources presented.

[c] Because the 5_{23}–4_{22} lines were upper limits on these sources, the R_{55} ratio placed no limits on the fit where the R_{33} and R_{35} ratios intersected; the χ^2 minima are underdetermined and effectively 0.

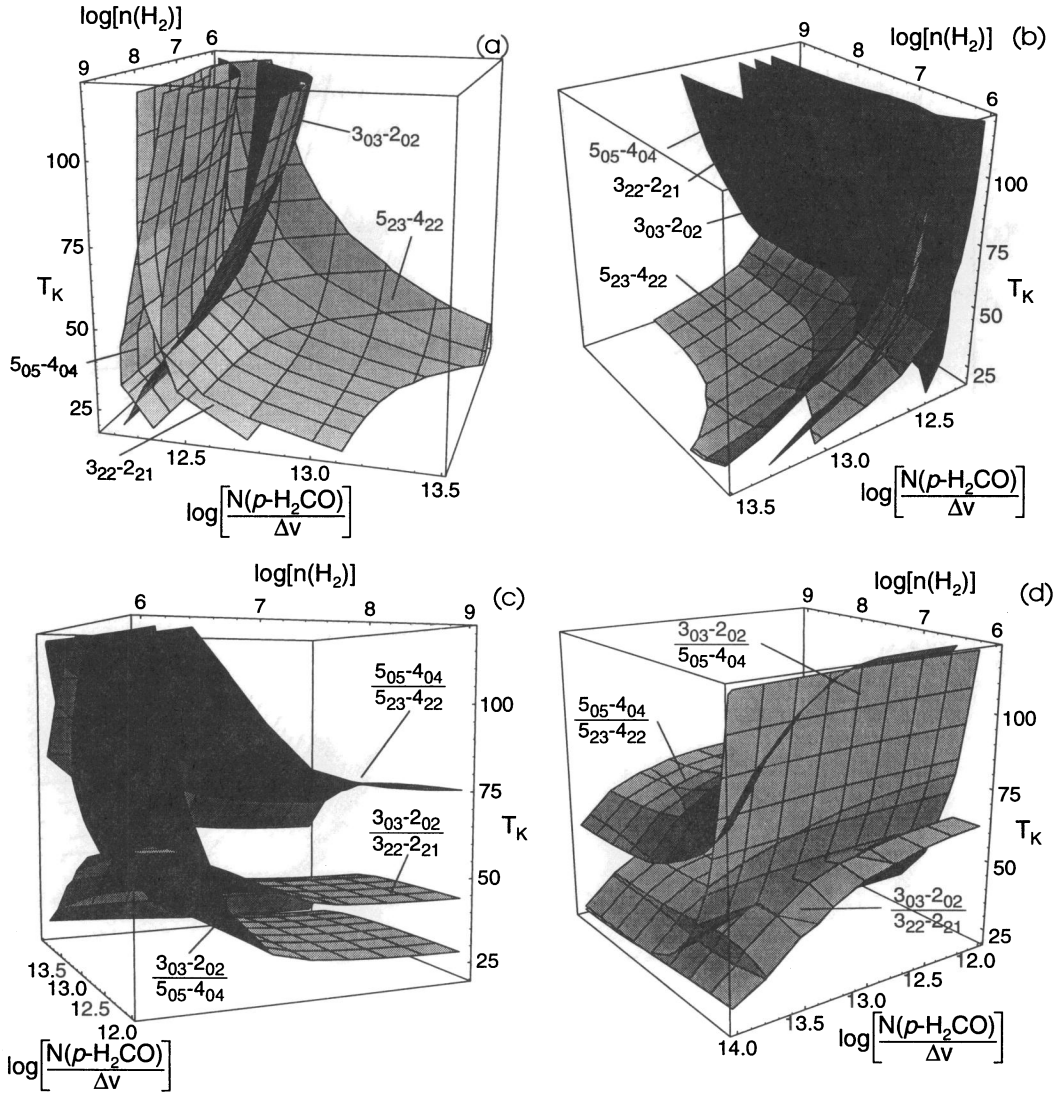

FIG. 2.—Line-ratio isosurfaces that indicate sets of values in T_K, $\log n_{H_2}$, and $\log [N(\text{para-}H_2CO)/\Delta v]$ parameter space consistent with our H_2CO observations of S68N. These isosurfaces are generated via LVG modeling, using the observed H_2CO line strengths and ratios. The surfaces intersect at values of gas parameters that are consistent with the data. *Top:* Two perspectives of the isosurfaces generated from peak line temperature observations. Note the well-constrained, narrow range of acceptable $\log [N(\text{para-}H_2CO)/\Delta v]$ values. *Bottom:* Two perspectives of the isosurfaces generated from ratios of observed line peaks for S68N. The two temperature-sensitive R_{33} and R_{55} line-ratio isosurfaces are clearly distinguished for this source.

4. DISCUSSION

4.1. *Warm and Cool* H_2CO *Components*

The strongest high-resolution 3_{03}–2_{02} spectra of the Serpens sources in Figure 1 are not simple Gaussian profiles, so we must consider whether there are multiple components that may affect the accuracy of our LVG models. There are clear dips in the profiles of the five strongest sources at $v_{LSR} \sim 8.5$ km s^{-1}, offset slightly from the line-center velocities of $v_{LSR} \sim 7.5$ km s^{-1} for all but FIRS 1. These features line up with the weaker emission in the ambient gas seen at IRS 53 and SVS 2. The simplest explanation for these dips is that they arise in a cool, absorbing layer in front of the sources and constitute self-reversals of the line.

A vexing problem, then, is determination of the optical depths of the cold, absorbing material. Our first step toward solution of this problem is to compare intensities of the 3 mm H_2CO and $H_2{}^{13}CO$ lines we have measured toward the three strongest submillimeter objects. The integrated $H_2CO/H_2{}^{13}CO$ line-intensity ratios for the 3 mm lines were 33 toward FIRS 1, 50 toward S68N, and over 100 toward SMM 4, which suggests that neither line has substantial optical depth toward FIRS 1 and that the H_2CO lines toward S68N and SMM 4 are relatively thin. The depth of the central feature in any of the 1 mm spectra is not large, which suggests optical depths in the cooler material of $\tau \sim 0.2$ at most (in FIRS 1).

We model the observed emission as the superposition of two components; a broad, warm component that underlies a cooler foreground component. The warm component, seen primarily in the 3_{03}–2_{02} transitions of Figure 1*a*, has a greater line width than the cool component, traced by the 1_{01}–0_{00} emission (e.g., 4.6 and 2.5 km s^{-1}, respectively, for S68N). The narrow, cool profiles are consistent with the absorption features, as discussed for the individual sources below.

As can be seen from the line profiles of Figure 1*a*, there is a substantial velocity offset between the absorption dip and the

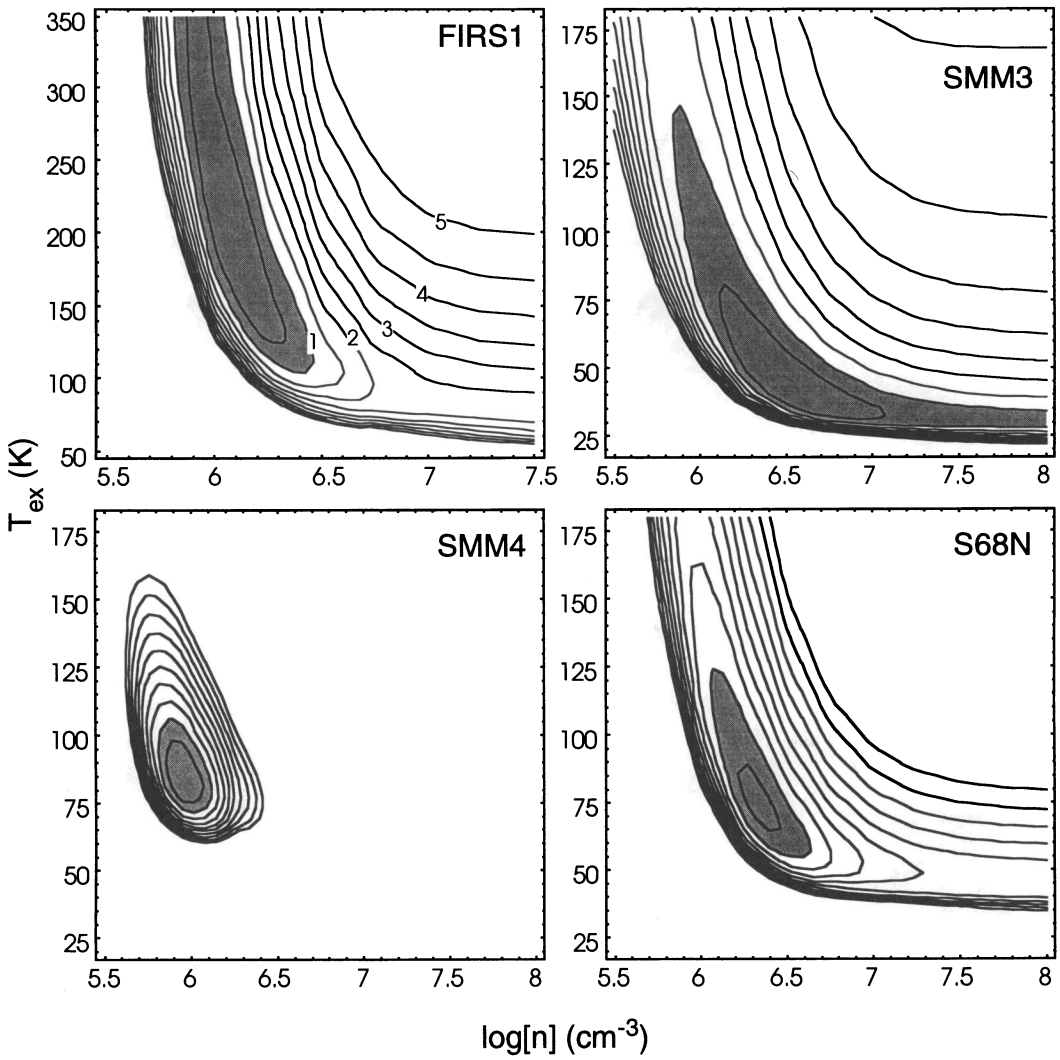

FIG. 3.—Minimization residuals of our LVG fits to multitransition H_2CO line data for the four Serpens sources FIRS 1, SMM 3, SMM 4, and S68N. For a single degree of freedom in these fits, the χ^2 values corresponding to 1 σ, 2 σ, and 3 σ levels are 1.1, 3.8, and 5.4, respectively. The 1 σ regions are highlighted in gray scale; the highest contours correspond to roughly the 3 σ level. Note the larger temperature scale used for FIRS 1/SMM 1.

line peak toward all sources, except, perhaps, for FIRS 1. Because of both this velocity offset and the narrow line profile of the foreground gas, the cool, foreground component does not substantially modify the peak intensities of the warm, background gas toward most of our observed sources. With the possible exception of FIRS 1 (as noted above), physical conditions derived for the warm gas component from the peak values of the CSO lines are unaffected by the presence of the cool, foreground component. A temperature gradient clearly must exist in the gas, with the more kinematically disturbed component also showing evidence of substantially warmer temperatures than the foreground gas. We discuss the offset between the cool and warm components at greater length in § 4.3.

4.2. *Serpens Submillimeter Sources*

4.2.1. *FIRS 1*

FIRS 1 has been studied extensively in recent years. Its triple radio-continuum source (Rodríguez et al. 1980) has been proposed as a possible proto–Herbig-Haro object (Curiel et al. 1993). The presence of a bipolar flow (for a recent discussion, see White et al. 1995) and water masers (Curiel et al. 1993) toward this object are well known, though the maser has been inactive recently (Wilking et al. 1994). With an overall observed luminosity of $\sim 50\ L_\odot$, it is the brightest submillimeter continuum source in the Serpens core.

McMullin et al. (1994) fitted the far-infrared and millimeter continuum fluxes from FIRS 1 as a modified blackbody with a 5″.6 source size, λ^{-2} emissivity law, and $T_{dust} \sim 32$–40 K. They noted the presence of excess 20–25 μm emission, "clearly indicating the presence of hotter dust." Torrelles et al. (1992) presented 4″ resolution maps of (1, 1) and (2, 2) NH_3 emission toward FIRS 1, from which they determined a rotational temperature of ~ 30 K, averaged over a region of 6″ radius. This suggests a kinetic temperature in agreement with the dust temperature determined by McMullin et al. (1994). The H_2CO we observe is highly excited, with gas kinetic temperatures in excess of 100 K. Since the gas and dust should be thermalized at the high densities we derive, the formaldehyde-emitting gas may be more closely associated with the luminosity source in the object, perhaps coincident with the 20–25 μm excess source

or with the centimeter continuum source(s). In a spherically symmetric source, the luminosity appears to be insufficient to maintain such warm gas temperatures over substantial distances. However, any image manifests the source aspherically, with a geometry such that a substantial column of cold dust and gas obscures the central object from our view, while outflow occurs nearly in the plane of the sky. Hence, the simple dust model may underestimate the true source luminosity, much of which may be emitted along the system's polar direction, absorbed and reemitted along the line of sight. Furthermore, since the VLA images attest to the existence and scale of ionized gas emission, it seems natural to expect warm, neutral gas in accompaniment. Velocity asymmetries in maps of H_2CO emission (Mangum et al. 1995) suggest that, indeed, the dense gas is affected by the flow.

To begin, we discuss the optical depth and relative placement of the warm and cooler H_2CO components toward FIRS 1. As we have mentioned, the isotopic ratio in the 3 mm lines suggests that moderate optical depths may occur very near line-center velocities. At FIRS 1, the 72 GHz H_2CO line-center emission velocity occurs at $v_{LSR} = 8.5$ km s^{-1} with a FWHM of 1.1 km s^{-1} (see Fig. 4*a*). There is modest agreement between the velocity of the 72 GHz $H_2{}^{13}CO$ line-center velocity and the velocity of the absorption dip (at $v_{LSR} = 8.95$ km s^{-1}) in the 218.222 GHz spectrum. The LSR velocity of the absorption dip in the 3_{03}–2_{02} spectrum toward FIRS 1 is redder than that of similar absorption dips that we observed toward other sources in this region.

Therefore, unlike the other strong submillimeter sources in Serpens, the self-reversal feature in FIRS 1 is nearly centered on the 3_{03}–2_{02} line and may affect the peak temperatures derived from our CSO observations. If the absorption feature is significantly stronger in the 3_{03}–2_{02} line than in the 3_{22}–3_{21} and 5_{05}–4_{04} lines, the corresponding R_{33} and R_{35} measurements could be off by (at most) a factor of 2, which would imply gas kinetic temperatures of $T_K \sim 70$ K. This lower kinetic temperature would be more in line with the kinetic temperatures derived from our LVG modeling of the other Serpens sources. Nevertheless, this still represents a significantly warmer component of gas than has previously been observed.

We next consider whether FIRS 1 appears to have

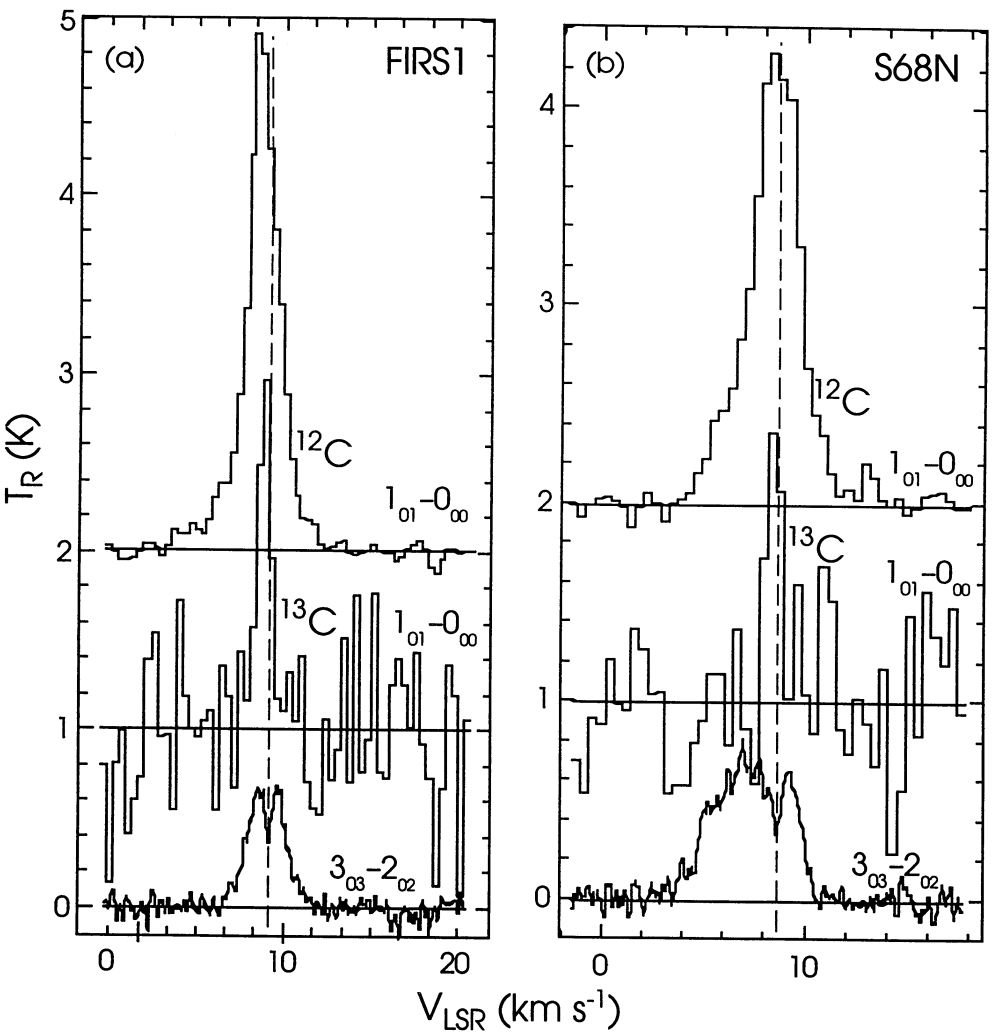

FIG. 4.—Emission from the H_2CO (1_{01}–0_{00}) and $H_2{}^{13}CO$ (1_{01}–0_{00}) transitions observed with the NRAO 12 m telescope and the H_2CO (3_{03}–2_{02}) transition observed with the CSO 10.4 m antenna. The $H_2{}^{13}CO$ 1_{01}–0_{00} spectra have been scaled up by a factor of 10. (*a*) Spectra for FIRS 1; (*b*) the corresponding spectra for S68N. The FIRS 1 spectra were taken at a slightly different B1950 position with the 12 m telescope ($18^h27^m17^s.5$, $+01°13'6''.5$) than CSO ($18^h27^m17^s.3$, $+01°13'23''$). The dashed vertical lines are aligned with the absorption features at $v_{LSR} = 8.95$ km s^{-1} in FIRS 1 and at $v_{LSR} = 8.46$ km s^{-1} in S68N.

assembled the bulk of its stellar mass. McMullin et al. (1994) found $0.5\ M_\odot \leq M \leq 3\ M_\odot$ as the limits on the central object's mass. The lower limit was derived under the assumptions of a mass accretion rate of $10^{-5}\ M_\odot\ \mathrm{yr}^{-1}$, of a protostellar radius of 3 $R_\odot$, and that the observed 50 $L_\odot$ luminosity is all accretion luminosity. The upper limit comes from the main-sequence mass of a star that would have a zero-age main sequence luminosity equivalent to the integrated luminosity that arises from FIRS 1. The derived mass of the compact (3800 AU diameter), $\lambda = 3.1$ mm continuum source depends on the chosen dust-emissivity law, from 0.8 $M_\odot$ for a λ^{-1} emissivity to 10 $M_\odot$ for a λ^{-2} emissivity. From our derived gas density of $1.3 \times 10^6\ \mathrm{cm}^{-3}$, we infer a total warm-gas mass of $\sim 0.25\ M_\odot$ for a uniform-density spherical cloud of 3800 AU diameter. Including the dominant cold gas component in the same area, we infer a total gas mass of 3 $M_\odot$. This gas-mass estimate is still subject to possible revision upward, as we do not yet know the true extent of the dense, cold gas component. FIRS 1 appears to be in its infall phase. We note that FIRS 1 is at a relatively early evolutionary stage, with a central source that is responsible for driving an outflow, powering H_2O masers, and heating the central, dense gas detected via our CSO H_2CO observations.

4.2.2. *S68N*

About 1.'5 north of FIRS 1, the source S68N is a particularly striking candidate protostar. Although evident as a distinct source in a variety of molecular tracers sensitive to dense gas (McMullin et al. 1994; White et al. 1995), it has only been detected as a diffuse continuum source at 1100 μm (Casali et al. 1993). Its close proximity to FIRS 1 makes it difficult to distinguish separately from this bright source in the *IRAS* data, although there is evidence for S68N's existing as a source blended with FIRS 1 at 50 and 100 μm in the contour maps of Zhang, Laureijs, & Clark (1988). However, HIRES-processed *IRAS* data provide a clear indication of a source associated with S68N at wavelengths longward of 12 μm.

Despite its low visibility at far-infrared (FIR) wavelengths, S68N presents a strong H_2CO 3_{03}–2_{02} line of integrated intensity 4.07 km s^{-1}. Our LVG analysis indicates the presence of warm gas with kinetic temperature $T_K \sim 75$ K and density $n_{H_2} \sim 2.5 \times 10^6\ \mathrm{cm}^{-3}$. Although not so drastic as the discrepancy for FIRS 1, this temperature is still much warmer than dust-temperature limits inferred for this region of $T_{\mathrm{dust}} \leq 20$ K (McMullin et al. 1994). Since the cool foreground component of gas is offset from the line center by ~ 1 km s^{-1}, we believe our determination of the warm-component gas conditions to be more reliable than those for FIRS 1. As with FIRS 1, an optically thick, cooler dust envelope could block signs of a warmer core. In molecular maps of the region in H_2CO 3_{03}–2_{02} and CS 3–2, S68N stands out as one of the two strongest sources of emission in the cloud core (Mangum et al. 1995). There is excellent agreement between the central velocities of the low-frequency $H_2{}^{13}CO$ and H_2CO lines and the velocity of the 3_{03}–2_{02} absorption dip, all of which occur at $v_{\mathrm{LSR}} = 8.46$ km s^{-1} (see Fig. 4*b*). The 71.0248 GHz $H_2{}^{13}CO$ line toward S68N has a narrow line width, 0.9 km s^{-1} FWHM, whereas the corresponding H_2CO line has a 3.85 km s^{-1} FWHM. A microtubulent model of the warm component of S68N indicates that the warm gas would contribute only a small amount to the H_2CO 1_{01}–0_{00} line profile, primarily in a blueshifted line wing, similar to what is observed (Fig. 5). The parameters of the cool component are not so well constrained as those of the warm component. The data are reasonably well fit by a microturbulent model characterized by a temperature of about 15 K, density $3 \times 10^5\ \mathrm{cm}^{-3}$, and H_2CO column density of $2 \times 10^{13}\ \mathrm{cm}^{-2}$.

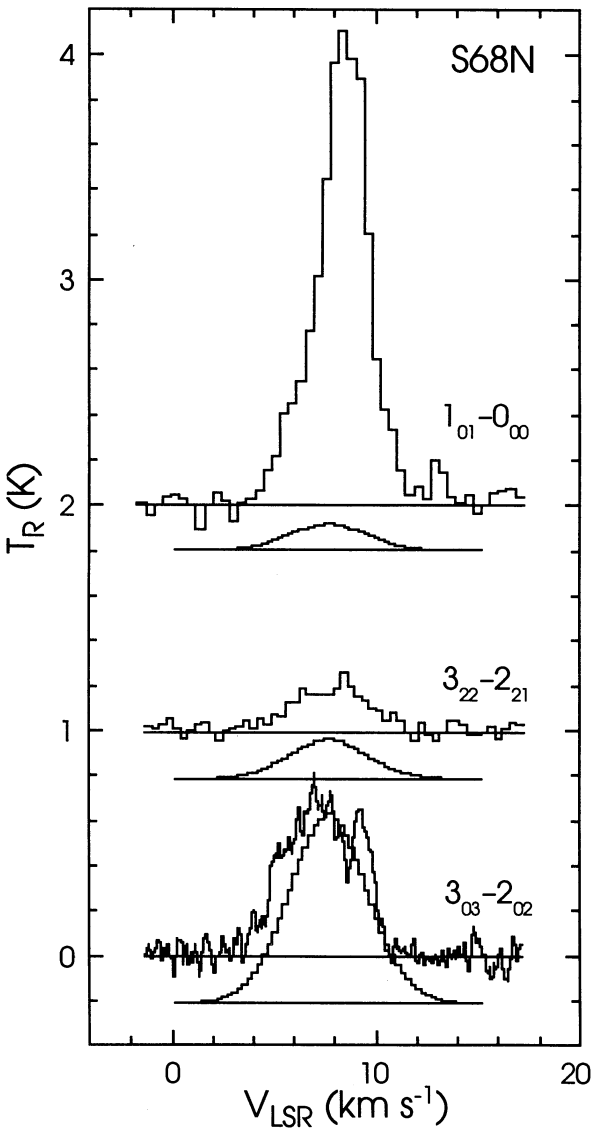

FIG. 5.—Sample microturbulent-model fitting to the H_2CO 3_{22}–2_{21}, 3_{03}–2_{02}, and 1_{01}–0_{00} transitions, using the warm-gas parameters presented in Table 2 for S68N as inputs. The model profiles agree well with the 218 GHz data but show that this warm component makes only a slight contribution to the 72 GHz line, primarily in its line wings. It is clear from this figure that the bulk of the 72 GHz line emission originates from a cooler gas component to which the 218 GHz line is relatively insensitive.

Although we find evidence for a localized warm component to the gas, is there other evidence that internal heating occurs, or might S68N be a preprotostellar clump without a central, accreting source? Bontemps et al. (1995) have observed the region of S68N in a deep 8.4 GHz image with the VLA. In their maps, no source coincides with S68N to within 3 σ limits of 0.12 mJy beam^{-1}. This flux limit does not strongly constrain the presence of a radio source at S68N; many of the sources detected by André, Montmerle, & Feigelson (1987) in Ophiuchus would not have been detected at this limit, given the distance to the Serpens cloud. White et al. (1995) found

some indication of high-velocity outflow gas near S68N, which suggests that a local driving source may be present. Likewise, Mangum et al. (1995) have found evidence for high-velocity molecular flows in H_2CO and CS around this source. In low-luminosity sources, though, the signature of a bipolar flow can be difficult to discover without interferometric measurements (see, e.g., Chandler et al. 1995). Even more compelling evidence is the recently discovered water maser emission from this region (Wootten 1995)—such emission is only found near regions of star formation. In low-luminosity regions, it frequently bears the spectral and spatial signature of a bipolar flow (e.g., IRAS 16293; Wootten 1992). We suggest that the water maser signals the presence of an undetected outflow from a young central source in S68N.

In order to estimate the luminosity of S68N, we combine upper limits to the FIR flux computed from *IRAS* HIRES images provided by IPAC[3] with the submillimeter continuum fluxes published by Casali et al. (1993). We place an upper limit on the total protostellar core luminosity of $L_* \leq 2\ L_\odot$ (this luminosity could be generated by a central protostar of mass $M_* \leq 0.02\ M_\odot$ undergoing pure accretion). We infer a warm-gas mass of $\sim 2.3\ M_\odot$ in this source (using $n_{H_2} = 2.5 \times 10^6$ cm^{-3} in a 10″ radius sphere). Since the inferred envelope mass is 2 orders of magnitude larger than the mass inferred for an embedded, accreting protostar, S68N appears to be a young Class 0 object that is at an extremely early stage of accretion.

4.2.3. *SMM 3*

The submillimeter source SMM 3 is located about 30″ west of the bright NIR nebulous source SVS 2. Although it does have some 2.2 μm emission, it is unclear whether this emission is associated directly with the submillimeter continuum source or is purely scattered light from SVS 2. There is no detectable 3 cm emission (≤ 22 μJy) within 10″ of the submillimeter position for SMM 3 (Bontemps et al. 1995). There is no obvious *IRAS* emission associated directly with this source at any band in the HIRES images we have examined. Nonetheless, low levels of emission could easily be confused with the bright emission from the nearby SVS 2. Using upper limits for the FIR fluxes derived from the HIRES maps and the submillimeter fluxes measured by Casali et al. (1993), we find an upper limit of $L_* \leq 11\ L_\odot$ for the intrinsic luminosity of SMM 3. If this luminosity originates purely from accretion, we then may infer a central source mass of $M_* \leq 0.1\ M_\odot$ for an assumed accretion rate of $10^{-5}\ M_\odot$ yr^{-1} onto a protostellar radius of 3 $R_\odot$. For comparison, a zero-age main sequence star with this luminosity would have a mass of 1.75 $M_\odot$.

The gas temperature inferred for SMM 3 is the lowest of all the Serpens sources we have observed, 40^{+110}_{-15} K, and it alone falls well within temperatures estimated for the surrounding dust (Zhang et al. 1988) and gas (McMullin et al. 1994) in the Serpens core. Along with the lowest derived temperature, SMM 3 also has the highest inferred gas density of any of the Serpens protostars we modeled. Neglecting the presence of any colder foreground component that may be present, we derive a gas mass of $\sim 2.9\ M_\odot$ from our CSO measurements (assuming a constant-density sphere of 10″ radius with $n_{H_2} \sim 10^{6.5}$). If there is indeed a central source in SMM 3, it would be among the youngest protostars known.

[3] The Infrared Processing and Analysis Center (IPAC) is funded by NASA as part of the *Infrared Astronomical Satellite* (*IRAS*) extended mission, under contract to JPL.

SMM 3 has not yet been extensively studied. Nevertheless, there is already some hint of an associated flow in CO (White et al. 1995). We note that our 218.222 GHz H_2CO line profile toward SMM 3 also exhibits broad, non-Gaussian wings. Determination of the actual kinematics of the line wing gas component awaits more sophisticated modeling. This same spectral line toward SMM 3 exhibits the absorption dip we have associated with cooler foreground gas toward S68N and FIRS 1. The developmental state of a star within SMM 3 remains uncertain until further follow-up observations can ascertain its status.

4.2.4. *SMM 4*

SMM 4 has the strongest overall H_2CO 3_{03}–2_{02} emission of all the observed submillimeter sources in Serpens, with an integrated intensity of 5.22 K km s^{-1}—the brightest source in this line; it also has the second-broadest wings after S68N. SMM 4 and S68N share a similarity in being sources of bright, localized emission in dense-gas tracers (in the H_2CO 3_{03}–2_{02} data presented here, CS 3–2 maps of the Serpens core [Mangum et al. 1995], and HCO^+ 3–2 [White et al. 1995]) while at the same time lacking substantial FIR emission. The *IRAS* 12 and 25 μm emissions near SMM 4 originate in the NIR clusters found to its northeast and southeast. Any intrinsic 60 or 100 μm emission from SMM 4 is highly confused with emission from these clusters (emission at both these wavelengths peaks at positions east of SMM 4, consistent with the locations of the clusters). As was the case with SMM 3, only limits can be placed on the spectral energy distribution of SMM 4 shortward of the 800 μm observations of Casali et al. (1993). Nevertheless, we have derived similar upper limits to the luminosity ($L \leq 11\ L_\odot$) of SMM 4. The 100 μm limit restricts the temperature that characterizes the spectral energy distribution to $T_{SED} \leq 20$ K.

Despite the icy character of the spectral energy distribution, evidence of stellar or protostellar activity is present. Bontemps et al. (1995) have located a 3 cm source near the millimeter position of SMM 4. In this crowded field, definite identification of the centimeter source with SMM 4 awaits further observations; nonetheless, the presence of the centimeter source suggests that SMM 4 contains an embedded energy source. Our data indicate that one component of the gas in SMM 4 has high temperatures and densities, with $T_K \sim 85$ K and $n_{H_2} \sim 10^{6.0}$ cm^{-3}. We note that SMM 4 has the lowest errors among our models, largely because of its strong 218 GHz lines (the generally weak 3_{22}–2_{21} line is one of the largest sources of error in the line ratios). This central, warm gas provides the second line of evidence of an energy source deep within SMM 4. Further evidence of energetic activity can be found in the H_2CO 3_{03}–2_{02} line profile (Fig. 1*a*), which has remarkably broad line wings, particularly on the blueshifted side. Moreover, strong evidence for a molecular outflow has been found by White et al. (1995) in CO, and a dense component of this flow has also been seen in H_2CO around this source (Mangum et al. 1995). Given reasonable estimates of the central and nearby masses from the gas and dust observations, the line width is too broad for a gravitational-infall explanation to be plausible; the flow probably proceeds outward from the central protostellar engine, which heats the gas and powers the centimeter continuum emission. The mass of warm gas in the envelope inferred from our density determination of $n_{H_2} = 10^6$ cm^{-3} within a 10″ radius sphere is $\sim 0.9\ M_\odot$, which suggests that only a fraction of the core mass has been warmed by the

central object. Overall, SMM 4 satisfies all the observational criteria required to classify it as a Class 0 protostar.

4.3. *Gas Infall*

The H_2CO (3_{03}–2_{02}) spectra of S68N, SMM 3, and SMM 4 all show striking similarities, particularly in asymmetry about their absorption features (see Fig. 1*a*). If we take the systemic velocity of the cloud to be that observed at the positions of IRS 53 and SVS 2 and in the H_2CO 1_{01}–0_{00} transitions, such an asymmetry is unexpected (see Fig. 4). The simple two-component model we have adopted of a cool foreground screen in front of a warm core suggests that S68N, SMM 3, and SMM 4 are all offset from the cloud velocity by ~ 1 km s^{-1}. That all the protostellar sources would happen to have the same peculiar velocity seems unlikely.

A possible explanation for this effect may be found in the characteristic spectral signature expected from gas infall onto a hot central source. Radiative-transfer models have shown that for a spherical cloud undergoing infall with progressively higher gas temperatures closer to the central source, the line profile for molecular gas in the cloud will be self-reversed and have a stronger blueshifted peak (Leung & Brown 1977; Walker et al. 1986; Zhou 1992). This model violates the LVG assumption since emission along a single line-of-sight velocity can originate from two distinct locations along the line of sight. Infall models have been applied to a number of protostellar sources in which this characteristic strong blueshifted emission component has been seen (Zhou & Evans 1994; Choi et al. 1995).

Our H_2CO profiles could be interpreted within this framework as evidence for gas infall for the sources S68N, SMM 3, and SMM 4. In the infall model, what we have so far referred to as the foreground, "cold" component is simply emission from the outermost portions of the infall envelope. This "cold" component dominates the core column density by factors of 3–5 over the warm gas in these sources. The infall model also predicts line-shape asymmetries, with the bulk of the line emission near the core center expected to originate from the warmer, blueshifted gas, as is observed. The apparent ~ 1 km s^{-1} blueshifted offset of the 218.222 GHz line profiles from the derived cloud rest velocity could derive, in part, from optical depth effects.

Although we do not discuss the Serpens submillimeter continuum source SMM 2 in any further detail in this paper, because of our lack of enough high-frequency line data to carry out an LVG analysis, we note here the similarity of its 218.222 GHz H_2CO line profile to those of the three potential infall sources mentioned above. SMM 2 is distinguished slightly from the previously discussed three sources in that most of its H_2CO 3_{03}–2_{02} line emission, as well as its absorption dip, seem to be blueshifted ~ 1 km s^{-1} relative to the other Serpens sources.

The profile of the FIRS 1 H_2CO 3_{03}–2_{02} line is unique among the Serpens submillimeter continuum sources in that it is completely symmetric about its self-reversal. In contrast to the other Serpens sources, the absorption dip in this line toward FIRS 1 is closely centered on the velocity of the ambient gas. Such a line profile is inconsistent with the asymmetric line profiles predicted by infall models and suggests the identification of FIRS 1 as a more evolved object than S68N, SMM 3, or SMM 4.

In order to test infall models, high spectral and spatial resolution maps will be required in several submillimeter H_2CO transitions toward SMM 2, SMM 3, SMM 4, and S68N. We also note that the Serpens sources show greater line asymmetries than protostellar sources modeled in recent work (Zhou & Evans 1994; Choi et al. 1995), which indicates that other factors that influence the line shapes (e.g., rotation and outflows) will have to be incorporated into future models.

5. SUMMARY

Because of its sensitivity to dense ($n_{H_2} \sim 10^6$–10^7 cm^{-3}), cold (10–100 K) gas, judiciously chosen millimeter and submillimeter line ratios of formaldehyde (H_2CO) provide an ideal probe of gas conditions in protostellar sources. We have obtained high velocity resolution spectra of the 3_{03}–2_{02} transition of H_2CO toward seven of the recently discovered submillimeter continuum sources in the Serpens cloud core, five of which have no NIR counterparts. Additional low velocity resolution spectra of the 3_{22}–2_{21}, 5_{05}–4_{04}, and 5_{23}–4_{22} transitions toward four sources, FIRS 1, S68N, SMM 3, and SMM 4 were used in an LVG analysis to derive gas temperatures and densities in these sources. We found high gas densities (1–3×10^6 cm^{-3}) toward all four sources and surprisingly high gas kinetic temperatures of 40 K (SMM 3), 75 K (S68N), 85 K (SMM 4), and 190 K (FIRS 1).

The high velocity resolution H_2CO 3_{03}–2_{02} line profiles toward SMM 2, SMM 3, SMM 4, S68N, and FIRS 1 all exhibit narrow absorption dips, which indicate the presence of cold, foreground absorbing gas. Additional NRAO 12 m observations of the 72 GHz lines of H_2CO and $H_2{}^{13}CO$ toward S68N and FIRS 1 confirm the presence of the cold foreground gas component. We have used a microturbulent code to derive the physical properties of the cold foreground gas and have shown that our derivation of the warm gas properties, for all but the FIRS 1 source, are unaffected by the presence of this gas.

Based on their high velocity resolution H_2CO 3_{03}–2_{02} line profiles, we suggest that four of the Serpens submillimeter continuum sources, SMM 2, SMM 3, SMM 4, and S68N, could be interpreted in the context of protostellar infall models. Based on our multitransition LVG analysis, in combination with *IRAS* HIRES data and submillimeter and millimeter continuum fluxes, we suggest that SMM 2, SMM 3, SMM 4, and S68N are most likely in the Class 0 stage of protostellar evolution, while FIRS 1 is most likely in the Class I stage.

Pending *Infrared Space Observatory* (*ISO*) observations of the Serpens core sources will aid in further constraining the evolutionary stage of these objects. Further progress in modeling the gas kinematics of the Serpens core dust continuum sources requires high spectral and spatial resolution maps in several submillimeter H_2CO transitions. Once these data are available, we intend to undertake more sophisticated modeling to improve on our current determination of gas conditions and to investigate infall models quantitatively.

We would like to thank Lee Mundy for early discussions leading to this project and Jeff Mangum and Joseph McMullin for enlightening conversations. We heartily but, sadly, posthumously thank Larry Strom of the Caltech Submillimeter Observatory, whose help at the telescope was indispensable. M. B. is indebted to Chris Purton for saving her life from severe altitude sickness while obtaining the data and would like to thank both Chris and Sandra Purton for their generous hospitality during her recovery.

REFERENCES

André, P., Montmerle, T., & Feigelson, E. D. 1987, AJ, 93, 1182
André, P., Ward-Thompson, D., & Barsony, M. 1993, ApJ, 406, 122
Anglada, G., Rodríguez, L. F., Cantó, J., Estalella, R., & Torrelles, J. M. 1992, ApJ, 395, 494
Barsony, M. 1994, in ASP Conf. Proc. 65, Clouds, Cores, and Low Mass Stars, ed. D. P. Clemens & R. Barvainis (San Francisco: ASP), 197
Barsony, M., Sasselov, D. D., Rucinski, S. M., Bloemhof, E. E., & Nyman, L.-Å. 1995, in preparation
Bertout, C. 1983, A&A, 126, L1
Bontemps, S., et al. 1995, in preparation
Casali, M. M., Eiroa, C., & Duncan, W. D. 1993, A&A, 275, 195
Chandler, C. J., Terebey, S., Barsony, M., & Moore, T. J. T. 1995, in Circumstellar Matter, ed. G. Watt (Dordrecht: Kluwer), in press
Choi, M., Evans, N. J., II, Gregersen, E. M., & Wang, Y. 1995, ApJ, 448, 742
Curiel, S., Rodríguez, L. F., Moran, J. M., & Cantó, J. 1993, ApJ, 415, 191
de Lara, E., Chavarria-K., C., & López-Molina, G. 1991, A&A, 243, 139
Eiroa, C., & Casali, M. M. 1992, A&A, 262, 468
Ellison, B. N., Schaffer, P. L., Schael, W., Vail, D., & Miller, R. E. 1989, Int. J. Infrared Millimeter Waves, 8, 937
Fletcher, A. B., & Stahler, S. W. 1994a, ApJ, 435, 313
———. 1994b, ApJ, 435, 329
Helmich, F. P., Jansen, D. J., De Graauw, Th., Groesbeck, T. D., & Van Dishoeck, E. F. 1994, A&A, 283, 626
Kutner, M. L., & Ulich, B. L. 1981, ApJ, 250, 341
Leung, C. M., & Brown, R. L. 1977, ApJ, 214, L73
Mangum, J. G. 1993, PASP, 105, 117
Mangum, J. G., Latter, W. B., & McMullin, J. P. 1995, in preparation
Mangum, J. G., & Wootten, A. 1993, ApJS, 89, 123
Mangum, J. G., Wootten, A., Loren, R. B., & Wadiak, E. J. 1990, ApJ, 348, 542
McMullin, J. P., Mundy, L. G., Wilking, B. A., Hezel, T., & Blake, G. A. 1994, ApJ, 424, 222
Rodríguez, L. F., Moran, J. M., Ho, P. T. P., & Gottlieb, E. W. 1980, ApJ, 235, 845
Torrelles, J. M., Gómez, J. F., Curiel, S., Eiroa, C., Rodríguez, L. F., & Ho, P. T. P. 1992, ApJ, 384, L59
Ulich, B. L., & Haas, R. W. 1976, ApJS, 30, 247
Walker, C. K., Lada, C. J., Young, E. T., Maloney, P. R., & Wilking, B. A. 1986, ApJ, 309, L47
White, G. J., Casali, M. M., & Eiroa, C. 1995, A&A, in press
Wilking, B. A., Claussen, M. J., Benson, P. J., Myers, P. C., Terebey, S., & Wootten, A. 1994, ApJ, 431, L119
Wootten, A. 1989, in IAU Colloq. 120, Structure and Dynamics of the Interstellar Medium, ed. G. Tenorio-Tagle, M. Moles, & J. Melnick (Berlin: Springer), 207
———. 1992, in Astrophysical Masers, ed. A. W. Clegg & G. E. Nedoluha (Berlin: Springer), 315
———. 1995, in preparation
Zhang, C. Y., Laureijs, R. J., & Clark, F. O. 1988, A&A, 196, 236
Zhou, S. 1992, ApJ, 394, 204
Zhou, S., & Evans, N. J., II. 1994, in ASP Conf. Proc. 65, Clouds, Cores, and Low Mass Stars, ed. D. P. Clemens & R. Barvainis (San Francisco: ASP), 183